



Published in final edited form as:

J Allergy Clin Immunol. 2017 December ; 140(6): 1651–1659.e1. doi:10.1016/j.jaci.2016.12.974.

Leucine-rich repeat containing 8A (*LRRC8A*)–dependent volume-regulated anion channel activity is dispensable for T-cell development and function

Craig D. Platt, MD, PhD^a, Janet Chou, MD^a, Patrick Houlihan, PhD^d, Yousef R. Badran, MD^a, Lalit Kumar, PhD^a, Wayne Bainter, BA^a, P. Luigi Poliani, MD, PhD^b, Carlos J. Perez, DVM, PhD^c, Sharon Y. R. Dent, PhD^c, David E. Clapham, MD, PhD^{d,e}, Fernando Benavides, DVM, PhD^{c,*}, and Raif S. Geha, MD^{a,*}

^aDivision of Immunology, Boston Children's Hospital, Harvard Medical School, Boston, Mass

^bDepartment of Molecular and Translational Medicine, University of Brescia, Brescia, Italy

^cDepartment of Epigenetics and Molecular Carcinogenesis, University of Texas M. D. Anderson Cancer Center, Smithville, and the Graduate School of Biomedical Sciences at Houston, Houston, Tex

^dDepartment of Cardiology, Boston Children's Hospital, Boston, Mass

^eHoward Hughes Medical Institute, Chevy Chase, Md

Abstract

Background—Leucine-rich repeat containing 8A (*LRRC8A*) is an ubiquitously expressed transmembrane protein with 17 leucine-rich repeats (LRRs) at its C-terminal end and is an essential component of the volume-regulated anion channel (VRAC), which controls cellular volume. A heterozygous mutation in *LRRC8A* that truncates the 2 terminal LRRs was reported in a patient with agammaglobulinemia and absent B cells and was demonstrated to exert a dominant negative effect on T- and B-cell development in mice. *Lrrc8a*^{-/-} mice have severely defective T-cell development and function. It is not known whether the T- and B-cell defects caused by *LRRC8A* deficiency are caused by loss of VRAC activity.

Objective—We sought to determine whether VRAC activity is required for normal T-cell development and function.

Methods—VRAC activity was examined by using patch-clamp analysis. Flow cytometry was used to examine T-cell development. T-cell proliferation, cytokine secretion, and antibody titers were measured by using standard techniques.

Corresponding author: Raif S. Geha, MD, One Blackfan Circle, Boston, MA 02115. raif.geha@childrens.harvard.edu.

*These authors contributed equally to this work.

Disclosure of potential conflict of interest: L. Kumar receives grant support from the Eleanor and Miles Shore 50th Anniversary Career Development Award. D. E. Clapham receives grant support from the Howard Hughes Medical Institute and serves as a consultant for Hydra Biosciences. R. S. Geha and J. Chou receives grant support from the National Institutes of Health. The rest of the authors declare that they have no relevant conflicts of interest.

The CrossMark symbol notifies online readers when updates have been made to the article such as errata or minor corrections

Results—We demonstrate that the spontaneous mouse mutant *ébouriffé* (*ebo/ebo*) harbors a homozygous 2-bp frameshift mutation in *Lrrc8a* that truncates the 15 terminal LRRs of LRRC8A. The *Lrrc8a^{ebo}* mutation does not affect protein expression but drastically diminishes VRAC activity in T cells. *ebo/ebo* mice share features with *Lrrc8a^{-/-}* mice that include curly hair, infertility, reduced longevity, and kidney abnormalities. However, in contrast to *Lrrc8a^{-/-}* mice, *ebo/ebo* mice have normal T-cell development and function and intact antibody response to T-dependent antigen.

Conclusion—LRRC8A-dependent VRAC activity is dispensable for T-cell development and function.

Keywords

Leucine-rich repeat containing 8A; volume-regulated anion channel; thymocyte development

Leucine-rich repeat containing 8A (*LRRC8A*) encodes an ubiquitously expressed 810-amino-acid cell-surface protein that spans the plasma membrane 4 times and contains 17 leucine-rich repeats (LRRs) in its C-terminal domain.^{1,2} LRRC8A has at least 2 biologic functions: it is critical for T-cell development³ and also is an essential component of the volume-regulated anion channel (VRAC), which is important for preserving constant cell volume in response to osmotic stress.^{4,5} VRAC has been implicated in a wide range of biological processes, including proliferation and cell survival.⁶ T cells were among the first cell types in which VRAC was identified,⁷ although it is unknown whether the VRAC activity of LRRC8A is necessary for T-cell development and survival.

LRRC8A was first identified through studies of a female patient with agammaglobulinemia and absent circulating B cells who was found to have a heterozygous mutation in *LRRC8A*. This mutation resulted in expression of a mutant protein, designated LRRC8A $\Delta^{91/35}$, in which the C-terminal two-and-a-half terminal LRRs were replaced by 35 novel amino acids encoded by intronic nucleotides.¹ The number and function of T cells in this patient were not reported. Irradiated wild-type (WT) mice reconstituted with syngeneic CD34⁺ cells transduced with the LRRC8A mutant had impaired T- and B-cell development.¹ Subsequently, we demonstrated that *Lrrc8a^{-/-}* mice had a striking phenotype characterized by significantly increased prenatal mortality, markedly reduced longevity, growth retardation, abnormal hair, sterility, and kidney abnormalities.³ Importantly, LRRC8A deficiency resulted in a severe block in early thymocyte differentiation and increased thymocyte apoptosis, resulting in markedly reduced thymic cellularity and severely impaired peripheral T-cell proliferation in response to T-cell receptor ligation.³ *Lrrc8a^{-/-}* \rightarrow *Rag2^{-/-}* bone marrow chimeras recapitulated the defects in thymocyte development and peripheral T-cell function, demonstrating that the T-cell defect in *Lrrc8a^{-/-}* mice is cell autonomous. Ligation of LRRC8A activates AKT, a kinase important for thymocyte survival, proliferation, and metabolism, through a LCK- ζ chain-associated protein of 70 kDa (ZAP-70)-GRB2-associated-binding protein 2 (GAB2)-phosphoinositide 3-kinase pathway.^{3,8} AKT phosphorylation was markedly reduced in the thymi of *Lrrc8a^{-/-}* mice.³ These findings established a critical role for LRRC8A in T-cell development.

VRAC is activated by conditions of low intracellular ionic strength, thereby permitting an efflux of anions that normalizes the osmotic gradient and restores cell volume.^{9,10} Knockdown of *LRRC8A* virtually abolishes VRAC activity in multiple cell types, including human T lymphocytes,^{4,5} demonstrating that LRRC8A, also known as SWELL1, is a necessary component of VRAC. Recent studies established that the pore-forming subunits of VRAC are composed of hexamers of LRRC8A and up to 4 LRRC8 family homologs (LRRC8B to LRRC8E).¹⁰ Because studies demonstrating the VRAC activity of LRRC8A were performed in transfected cell lines, the contribution of LRRC8A-driven VRAC activity to physiologic processes remains undetermined.

We report here that the spontaneous mouse mutation designated *ébouriffé* (*ebo*) is caused by a 2-bp deletion in *Lrrc8a* that results in truncation of the 15 C-terminal LRRs of LRRC8A and a dramatic reduction of VRAC activity in T cells. Like *Lrrc8a*^{-/-} mice, *ebo/ebo* mice have reduced survival, abnormal hair, infertility, and abnormal renal tubular morphology.³ In contrast to *Lrrc8a*^{-/-} mice, *ebo/ebo* mice have intact T-cell development and function. Thus the critical role LRRC8A plays in T-cell development and function is independent of its VRAC activity.

METHODS

Mice

FVB/N.Cg-*ebo* (N10) congenic mice,¹¹ *Lrrc8a*^{-/-} mice,³ CD4 Cre *Lrrc8a*^{fl/fl} mice, and their WT littermates were kept in microisolator cages under specific pathogen-free conditions. The *ebo* mutant allele was backcrossed onto the FVB/N background for 10 generations (partially by using marker-assisted backcrossing). All procedures were performed within the guidelines of the Animal Care and Use Committee of Boston Children's Hospital.

Semiquantitative RT-PCR

Total RNA was prepared from splenocytes of WT and *ebo/ebo* mice by using the RNeasy kit (Qiagen, Hilden, Germany). cDNA synthesis and amplification were performed from total RNA by using the Superscript III One Step RT-PCR System with Platinum Taq DNA polymerase (Thermo Fisher, Waltham, Mass). Primers used for *Lrrc8a* were as follows: forward primer, 5'-TCACAGCCAATAGGATTGAAGC-3' (spans exons 3 and 4); reverse primer, 5'-CCTAGCCCAGTGCCAATAAG-3' (exon 4). The following primers for *18S* were used as a control: forward primer, 5'-CGGCTACCACATCCAAGGAA-3'; reverse primer, 5'-GCTGGAATTA CCGCGGCT-3'.

Preparation of cells and flow cytometry

Single-cell suspensions from thymi and spleens of 3- to 11-week-old mice were prepared by disrupting tissue and passing through a 70 µm-cell strainer (Falcon; Thermo Fisher Scientific). Cells were stained with the appropriate fluorochrome-labeled mAbs and analyzed on an LSRFortessa (BD Biosciences, San Jose, Calif). Antibodies were purchased from eBioscience (San Diego, Calif), unless otherwise indicated. Splenocyte and thymocyte subsets were defined by using fluorescently labeled antibodies against CD3 (clone145-2C11), CD4 (clone RM4-4), CD8 (clone 53-6.7), and B220 (clone RA3-6B2).

Lineage-negative cells were identified by excluding cells stained with a single fluorochrome-labeled cocktail of phycoerythrin-labeled CD19 (BD, clone 1D3), CD3 (clone 145-2C11), CD4 (clone GK1.5), CD8 (clone 53-6.7), CD11b (clone M1/70), CD11c (clone N418), Ly6 (clone HK1.4), NK1.1 (clone PK136), T-cell receptor $\gamma\delta$ (BD, clone GL3), and Ter-119 (clone Ter119) to distinguish thymocyte progenitors. Cells were subsequently stained with fluorescently labeled mAbs to CD44 (clone IM-7) and CD25 (clone PC61; BioLegend, San Diego, Calif).

Immunoblotting and flow cytometric analysis of LRRC8A expression

A polyclonal antibody (C18) was raised in rabbits against an 18-amino-acid sequence (amino acids 791-808) at the C-terminus of LRRC8A and affinity purified, as previously described.³ Cell lysates were immunoblotted with C18 or anti-actin (clone ACTN05 [C4]; Abcam, Cambridge, United Kingdom), followed by horseradish peroxidase-conjugated goat anti-rabbit antibody or horseradish peroxidase-conjugated goat anti-mouse antibody. Intracellular flow cytometric staining was done per the instructions provided with the Cytoperm/Cytofix Cell Permeabilization and Staining Kit (BD Biosciences). Cells were stained with a rabbit antibody against the amino acid sequence 87 to 104 in the N-terminus of LRRC8A (anti-LRRC8A₈₇₋₁₀₄) before detection with fluorescein isothiocyanate-labeled anti-rabbit antibody (BD Biosciences).

Electrophysiology

Splenic T cells were purified by means of negative selection (Miltenyi Biotech, Bergisch Gladbach, Germany). Peritoneal macrophages were obtained by means of peritoneal lavage with ice-cold PBS. T cells and macrophages were cultured for 2 days. Current traces were acquired after initiation of 220-mOsm saline perfusion normalized to membrane capacitance. Whole-cell patch-clamp recordings were performed with an Axopatch 200B amplifier, Digidata 1320A analog-to-digital converter, and pClamp 9.2 software (Molecular Devices, Sunnyvale, Calif). Digital acquisition was performed at a 10-kHz sampling frequency; voltage-clamped data were low-pass filtered at 1 kHz. A whole-cell patch clamp was performed with thick-walled, borosilicate glass micropipettes pulled to a pipette resistance of 3 to 4 M Ω . Series resistance was compensated to 80%. Cells were held at -70 mV with voltage ramps from -100 mV to +100 mV over 400 ms at 5-second intervals. Currents were measured at -80 and +80 mV to plot time courses. Voltage steps were from -70 to +140 mV at +10-mV intervals (step duration, 40 ms). Voltage steps were recorded at 5 minutes after shift to hypotonic solution for T cells and 12 minutes for macrophages. All recordings were performed at approximately 22°C. Internal pipette solution consisted of the following: 120 mmol/L CsASP, 10 mmol/L Cs₄BAPTA, 4mmol/L MgATP, 2mmol/L MgCl₂, 8mmol/L NaCl, and 10 mmol/L HEPES (pH 7.2 with CsOH). External bath solution (220 mOsm) consisted of the following: 95 mmol/L NaCl, 2 mmol/L CaCl₂, 1 mmol/L MgCl₂, 5 mmol/L CsCl, 10 mmol/L HEPES, and 10 mmol/L glucose (pH 7.4 with NaOH), with 100 mmol/L mannitol added to yield 320-mOsm solutions.

Histopathology

Thymic morphology and expression of specific markers was assayed by using both routine hematoxylin and eosin staining and immunohistochemistry with 2- μ m-thick formalin-fixed, paraffin-embedded thymic sections, as described previously.³

In vitro proliferation and activation of splenic T cells

Purified splenic T cells were labeled with CellTrace Violet (Life Technologies, Grand Island, NY) before culture in medium alone or in wells with plate-bound anti-CD3 mAb (clone KT3; Abcam) with or without anti-CD28 mAb (clone L293; BD Biosciences) or 40 ng/mL IL-2 (PeproTech, Rocky Hills, NJ). Phorbol 12-myristate 13-acetate (Sigma-Aldrich, St Louis, Mo) was used at 50 ng/mL, and ionomycin (Sigma-Aldrich) was used at 0.5 μ mol/L. Harvested cells were labeled with anti-CD4-phycoerythrin (clone RM4-4, eBioscience), and proliferation was assessed by measuring dilution of CellTrace violet using flow cytometry with an LSRFortessa (BD Biosciences). IL-2 and IFN- γ concentrations in supernatants were measured by using ELISA (Ready-SET-Go!; eBioscience).

Immunization and assessment of T- and B-cell responses

Two-month-old mice were immunized intraperitoneally with 10 μ g of TNP-KLH (Biosearch Technologies, Petaluma, Calif) and Imject Alum (Thermo Fisher Scientific). Mice were subsequently boosted on day 14 with 2.5 μ g of TNP-KLH and Imject Alum. Splenocytes were harvested on day 21, labeled with CellTrace Violet (Life Technologies) and cultured at a concentration of 3×10^5 cells in the presence of media alone or KLH at the indicated concentration. On day 3, supernatants were harvested, and IL-2 and IFN- γ levels were measured by means of ELISA (Ready-SET-Go!; eBioscience). Levels of antigen-specific antibody responses from serum obtained on days 0 and 21 were analyzed by using TNP-specific ELISA with 96-well plates coated with TNP-conjugated BSA (Biosearch Technologies) at 10 μ g/mL in PBS. Plates were coated with TNP/BSA conjugated at a molar ratio of 2:1 to detect high-affinity antibody and TNP/BSA at a molar ratio of 32:1 to detect low-affinity antibody. Sera were diluted at 1:300, 1:1,000, 1:3,000, 1:9,000, 1:27,000, and 1:81,000. KLH-specific antibodies were detected with IgG-alkaline phosphatase. PNPP Substrate (Sigma) was added, and OD 405 was determined with a microplate reader (Molecular Devices).

Statistical analysis

Statistical analysis of the data with the Student *t* test was performed with Prism software (GraphPad Software, La Jolla, Calif).

RESULTS

***ebo/ebo* mice have a homozygous frameshift mutation in *Lrrc8a* and share phenotypic features with *Lrrc8a*^{-/-} mice**

The *ebo* autosomal recessive mutation arose spontaneously in a substrain of BALB/c mice.¹¹ Positional cloning localized the mutation to a region in mouse chromosome 2 (between D2Mit153 and D2Mit64, 29.27-31.20 Mb) homologous with human chromosome 9q34,

which includes *LRRC8A*. Next-generation DNA sequencing of this interval revealed a homozygous 2-bp deletion in exon 3 of *Lrrc8a* in *ebo/ebo* mice (Fig 1A). No other mutations were detected. The *ebo* frameshift mutation in *Lrrc8a* (c.1325_1326delTA:p.F443*) is predicted to result in a truncated LRRC8A₁₋₄₄₂ protein (LRRC8A^{ebo}) that lacks the 15 terminal LRRs (LRR3–LRR17) but retains all 4 transmembrane (TM) domains and the first 2 LRRs. RT-PCR analysis of splenocytes revealed that *Lrrc8a* mRNA expression levels were comparable in *ebo/ebo* mice and WT littermates (Fig 1B), indicating that the *ebo* mutation does not alter *Lrrc8a* mRNA stability.

We next examined the effect of the mutation on the expression of the LRRC8A mutant protein. As expected, immunoblotting with an antibody raised against a sequence at the C-terminal end of LRRC8A (anti-LRRC8A₇₉₁₋₈₀₈) revealed robust expression of LRRC8A in WT splenocytes but no detectable expression of LRRC8A in cells from *ebo/ebo* mice (Fig 1C). The N-terminal region of LRRC8A shows a high degree of homology with other LRRC8 family members (LRRC8B, LRRC8C, LRRC8D, and LRRC8E). The 2 available commercial antibodies against the N-terminus of LRRC8A, anti-LRRC8A₁₋₅₀ (Sigma) and anti-LRRC8A₅₀₋₁₀₀ (Bethyl Laboratories, Montgomery, Tex), showed no selectivity for LRRC8A because they stained T cells from WT and *Lrrc8a*^{-/-} mice equally well (data not shown). Subsequently, we raised a rabbit antibody against the amino acid sequence 87 to 104 located between TM1 and TM2 in the N-terminus of LRRC8A because this sequence showed the least homology with the corresponding amino acid sequences in other LRRC8 family members among regions with suitable antigenicity (Fig 1D). Nevertheless, this homology ranged from 22% for LRRC8E to 39% for LRRC8B. Intracellular staining with anti-LRRC8A₈₇₋₁₀₄ antibody yielded a significantly lower mean fluorescence intensity in T cells from *Lrrc8a*^{-/-} mice compared with those from WT control mice (474.9 ± 610.73 vs 631.2 ± 28.3, n = 6, *P* < .001; Fig 1, E, left panel). This incomplete loss of signal in *Lrrc8a* knockout cells is likely due to cross-reactivity with other LRRC8 family members. In contrast, there was no significant shift in the mean fluorescence intensity of T cells from *ebo/ebo* mice and WT control mice (318.7 ± 42.1 vs 330.1 ± 79.2, n = 5, *P* = .89; Fig 1E, right panel). These results suggest that the LRRC8A^{ebo} mutant is expressed in T cells from *ebo/ebo* mice. Taken together, these results indicate that the *ebo* mutation leads to deletion of the C-terminus of LRRC8A but does not appear to affect the expression level of the truncated protein.

As previously reported,¹¹ *ebo/ebo* mice have wavy hair and curled vibrissae, features also shared by *Lrrc8a*^{-/-} mice (Fig 2A).³ The frequency of live *ebo/ebo* pups among 124 pups obtained from matings of *+/ebo* heterozygotes was 22%, which was close to the expected Mendelian frequency of 25%. This is in contrast to the 5.5% frequency of live *Lrrc8a*^{-/-} pups obtained from mating *Lrrc8a*^{+/-} heterozygotes.³ *ebo/ebo* mice were sterile, like *Lrrc8a*^{-/-} mice. In contrast to *Lrrc8a*^{-/-} mice, which have severe growth impairment,³ the weight of *ebo/ebo* mice was comparable with that of WT littermates (Fig 2B). Nevertheless, *ebo/ebo* mice had significantly decreased survival compared with WT littermates, with only 60% reaching the age of 100 days (Fig 2C). This survival is significantly longer than that of *Lrrc8a*^{-/-} mice, all of which die by 100 days of age.³ Histologic examination of organs from *ebo/ebo* mice revealed hepatocellular swelling in the liver, atrophy of the secretory convoluted ducts in the submandibular gland, and tubular degeneration in the kidneys, which

is also observed in *Lrrc8a*^{-/-} mice (Fig 2D).³ Histology of the skin and gonads in *ebo/ebo* mice was also similar to that of *Lrrc8a*^{-/-} mice³ and will be detailed in a separate publication. *ebo/ebo* mice, unlike *Lrrc8a*^{-/-} mice, had normal striated muscle histology (data not shown). Heterozygous *+ebo* mice, like heterozygous *Lrrc8a*^{+/-} mice, appear phenotypically identical to WT littermates (Fig 2A). The phenotypic characteristics shared by *ebo/ebo* and *Lrrc8a*^{-/-} mice provide strong evidence that the 2-bp deletion in *Lrrc8a* is causative of the *ebo/ebo* phenotype.

The *ebo* mutation severely impairs VRAC activity in T cells

VRAC activity was measured by using whole-cell voltage clamp recordings of cells subjected to 220 mOsm of hypo-osmotic stress with the solution scheme outlined in Fig 3A. Voltage step analysis of currents in splenic T cells from C57BL/6 and FVB/N mice showed delayed activation, outward rectification, and desensitization during strong depolarization, features characteristic of VRAC (Fig 3B, left panel). Currents were severely diminished in *ebo/ebo* T cells (Fig 3B, right panel). Current density (current normalized to capacitance to account for differences in cell size), which is representative of VRAC activity in response to hypo-osmotic stress, was readily detectable in T cells from C57BL/6 and FVB/N mice, with no significant difference between the 2 strains (Fig 3C). In contrast, current density was drastically diminished in T cells from both *Lrrc8a*^{-/-} mice (C57BL/6 background) and *ebo/ebo* mice (FVB/N background), demonstrating that full-length LRRC8A, including the 15 terminal LRRs, is essential for normal VRAC activity in T cells (Fig 3C). The virtually absent current density in *Lrrc8a*^{-/-} T cells is consistent with the critical role of LRRC8A in VRAC activity.^{4,5} Importantly, there was no significant difference between *Lrrc8a*^{-/-} and *ebo/ebo* mice in the residual current density measured at -80 mV, which closely approximates the 270 mV resting membrane potential under physiologic conditions. When analyzed at 180 mV, the residual VRAC activity was slightly higher in *ebo/ebo* T cells than in *Lrrc8a*^{-/-} T cells, suggesting that LRRC8A^{ebo} can contribute to the residual VRAC activity induced under such nonphysiologic conditions in T cells.

Peritoneal macrophages from *Lrrc8a*^{-/-} and *ebo/ebo* mice also had drastically reduced VRAC activity, indicating that the *ebo* mutation affects VRAC activity in cell types other than T cells (Fig 3D and E). There was no significant difference in residual VRAC activity between *ebo/ebo* and *Lrrc8a*^{-/-} macrophages at -80 or +80 mV. T cells and peritoneal macrophages from *+ebo* heterozygous mice exhibited normal VRAC activity with kinetics comparable with those of WT cells (data not shown).

Normal T-cell development and function in *ebo/ebo* mice

Lrrc8a^{-/-} mice exhibit a severe cell-intrinsic defect in thymocyte development, with a 10-fold reduction in thymic cellularity, a block in thymocyte development at the double-negative 2 (DN2) stage, and decreased phosphorylated AKT content.³ Thymi from *Lrrc8a*^{-/-} mice exhibit effacement of the corticomedullary junction, numerous pyknotic nuclei and abnormal distribution of cortical thymic epithelial cells and medullary thymic epithelial cells (mTECs).³ Therefore, we examined T-cell development in *ebo/ebo* mice to determine whether this was affected by dramatically reduced VRAC activity. Thymic size and cellularity were comparable in *ebo/ebo* mice and WT littermates (Fig 4A and B).

Furthermore, thymi from *ebo/ebo* mice had a normal corticomedullary junction with no increase in numbers of pyknotic nuclei (Fig 4C) and normal numbers and distribution of terminal deoxynucleotidyl transferase–positive immature thymocytes and CD3⁺ maturing thymocytes (see Fig E1 in this article’s Online Repository at www.jacionline.org). The thymi of *ebo/ebo* mice had normal numbers and distribution of cytokeratin 8⁺ cortical thymic epithelial cells and cytokeratin 5⁺ mTECs, and their mTECs showed normal expression of *Ulex europaeus* agglutinin and the autoimmune regulator protein (see Fig E1). The percentages of DN, double-positive, and single-positive thymocytes, as well as DN1-DN4 thymocytes, were comparable in *ebo/ebo* mice and WT littermates (Fig 4D and E). Furthermore, phospho-AKT in the thymus of *ebo/ebo* mice was comparable with that in WT littermates (Fig 4F). Splenic cellularity, T- and B-cell numbers, and CD4⁺/CD8⁺ T-cell subset distribution were comparable between *ebo/ebo* mice and WT littermates (Fig 4, G–I). Overall, there was no detectable defect in thymocyte maturation.

We next assessed T-cell function because we demonstrated previously that *Lrrc8a*^{-/-} mice and *Lrrc8a*^{-/-} → *Rag2*^{-/-} chimeras have significantly impaired splenic T-cell proliferation and IL-2 secretion in response to immobilized anti-CD3.³ In contrast, the proliferation of splenic T cells in response to anti-CD3, anti-CD3 plus anti-CD28, and anti-CD3 plus IL-2 was comparable between *ebo/ebo* mice and WT littermates (Fig 5A). Furthermore, IL-2 and IFN- γ production by splenic T cells after stimulation with immobilized anti-CD3 mAb was comparable in the 2 strains (Fig 5B and C).

We next assessed the T-cell response to immunization with the T-dependent antigen TNP-KLH. Splenic T-cell proliferation and cytokine secretion in response to *in vitro* restimulation with KLH were comparable in *ebo/ebo* mice and WT littermates (Fig 5, D–F). Furthermore, the titers of both high- and low-affinity anti-TNP IgG antibodies were comparable in the 2 strains (Fig 5G and H). The normal T-dependent antibody response of *ebo/ebo* mice, together with the previously demonstrated normal T-independent antibody response in *Lrrc8a*^{-/-} mice, suggest that VRAC activity is not essential for B-cell function.

DISCUSSION

We demonstrate that *ebo/ebo* mice, which express a truncated LRRC8A mutant that virtually lacks VRAC activity, have normal T-cell development and function but retain some of the phenotypic features of LRRC8A^{null} mice. These findings demonstrate that LRRC8A-dependent VRAC activity is dispensable for T-cell development and function.

It is important to note that when the VRAC activity of T lymphocytes and peritoneal macrophages was evaluated in response to osmotic stress at –80 mV, which approximates resting membrane potential, there was dramatic reduction in VRAC activity similar to that seen in *Lrrc8a*^{-/-} mice. This finding strongly suggests that under physiologic conditions, the 15 terminal LRRs that are deleted in the LRRC8A^{ebo} mutant are necessary for VRAC activity. In a previous study, the LRRC8A^{91/+35} mutant, in which the two and a half terminal LRRs are replaced by 35 novel amino acids encoded by intronic nucleotides, did not generate a VRAC current.⁴ The observation that in contrast to LRRC8A^{ebo}, LRRC8A^{91/+35} perturbed T- and B-cell development, suggests that the added 35 amino

acids rather than loss of VRAC activity might have played an important role in the effect exerted by the LRRC8A^{91/135} mutant on T and B cells.

Given the dramatic defects in T-cell development and function in *Lrrc8a*^{-/-} mice, it was surprising to find that *ebo/ebo* mice, which virtually lacked VRAC activity, had normal thymocyte development, normal thymus morphology, and normal *in vitro* and *in vivo* T-cell function. This suggests a role for LRRC8A in T-cell development function that is distinct from its role in the regulation of cellular volume. We previously found that ligation of LRRC8A results in AKT phosphorylation in thymocytes.³ Furthermore, a GST-LRRC8A₃₄₃₋₈₁₀ fusion protein containing all 468 C-terminal amino acids that follow the TM4 region bound to TECs and to the OP9-DL1 cell line and inhibited OP9-DL1-driven maturation of DN thymocytes into double-positive thymocytes,³ suggesting that amino acids 343 to 810 of LRRC8A are important for T-cell development. However, because LRRC8A might multimerize through its LRR repeats,¹² we cannot rule out the possibility that another region of LRRC8A binds to the putative ligand and that inhibition by GST-LRRC8A₃₄₃₋₈₁₀ is due to steric effects. Further experiments are needed to precisely map the region of LRRC8A that interacts with its putative ligand.

Epitope-tagging studies suggest that both N- and C-termini might be intracellular.^{4,5} However, studies with antibodies directed at the C-terminus of LRRC8A and the loop between the TM2 and TM3 regions clearly indicate that a fraction of LRRC8A is inserted in the cell membrane in the opposite orientation, in which both the N- and C-termini are extracellular.³ Dual-membrane topology has been described for a number of other proteins that span the plasma membrane 4 times,¹³ and the available evidence³⁻⁵ supports such a model for LRRC8A (Fig 6). We suggest that when the N- and C-termini of LRRC8A are extracellular (Fig 6A, orientation A) the LRR-containing C-terminal region is extracellular and available to interact with the putative LRRC8A ligand, resulting in GRB2-LCK-ZAP-70-mediated activation of AKT and thymocyte survival. In contrast, when the N- and C-termini are intracellular (Fig 6B, orientation B), the LRR-containing C-terminal region of LRRC8A is intracellular and might mediate VRAC activity (Fig 6B).

In summary, we have identified a hypomorphic mutation in *Lrrc8a*, *Lrrc8a*^{ebo}, that dramatically reduces VRAC activity but spares T-cell development and function. Although VRAC activity was virtually negligible in T cells from both *ebo/ebo* and *Lrrc8a*^{-/-} mice under physiologic voltage conditions, unlike *Lrrc8a*^{-/-} mice, which demonstrate a severe defect in T-cell development, *ebo/ebo* mice had intact T-cell development. This leads us to conclude that the role played by LRRC8A in T cells is independent of its role in regulating cellular volume.

Supplementary Material

Refer to Web version on PubMed Central for supplementary material.

Acknowledgments

Supported by AI083503 (to R.S.G.), T32 AI007512 (to C.D.P.), K08AI116979 (to J.C.), R21 AI079769, the Eleanor and Miles Shore 50th Anniversary Career Development Award (to L.K.), and NCI/CA016672 (to F.B.).

Abbreviations

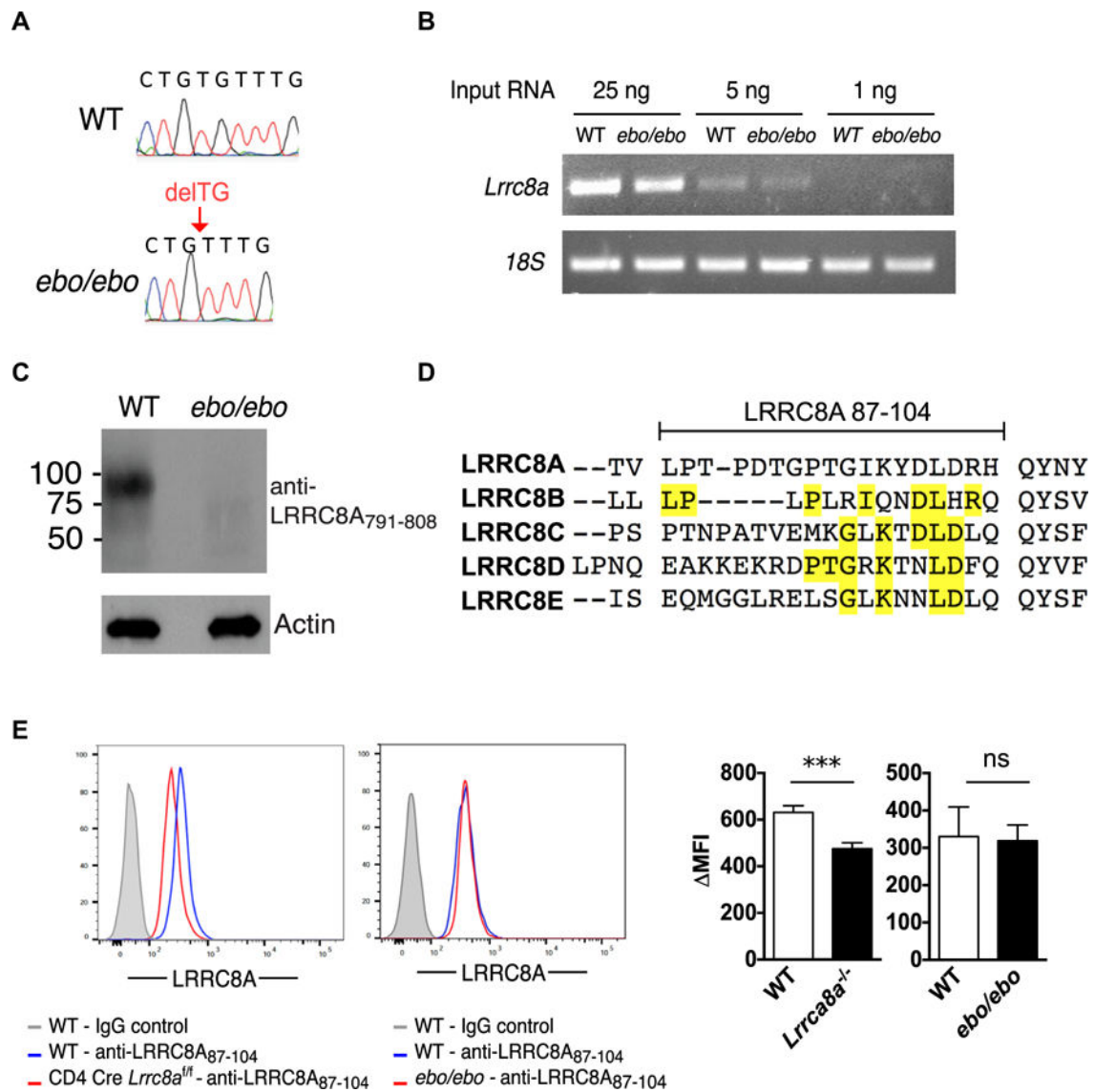
DN	Double negative
LRR	Leucine-rich repeat
LRRC8A	Leucine-rich repeat containing 8A
mTEC	Medullary thymic epithelial cell
TM	Transmembrane
VRAC	Volume-regulated anion channel
WT	Wild-type
ZAP-70	ζ Chain-associated protein of 70 kDa

References

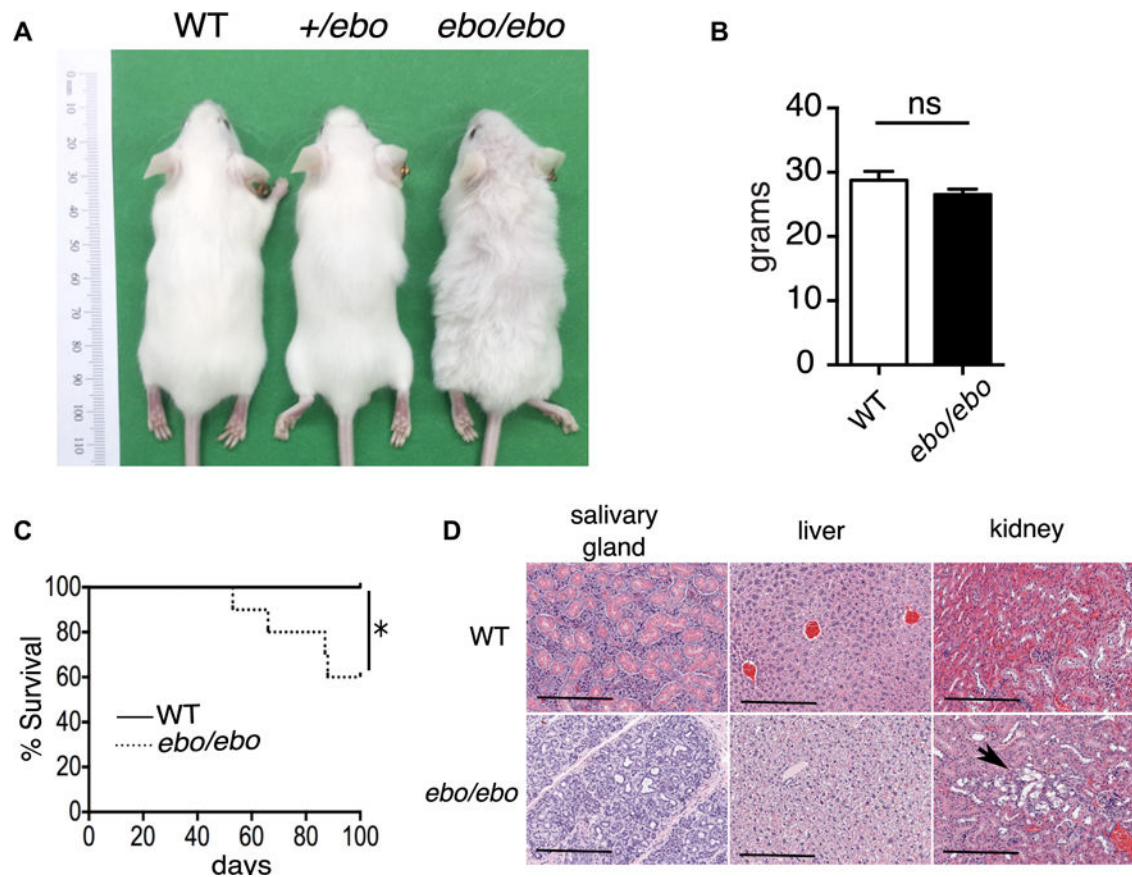
1. Sawada A, Takihara Y, Kim JY, Matsuda-Hashii Y, Tokimasa S, Fujisaki H, et al. A congenital mutation of the novel gene LRRC8 causes agammaglobulinemia in humans. *J Clin Invest*. 2003; 112:1707–13. [PubMed: 14660746]
2. Smits G, Kajava AV. LRRC8 extracellular domain is composed of 17 leucine-rich repeats. *Mol Immunol*. 2004; 41:561–2. [PubMed: 15183935]
3. Kumar L, Chou J, Yee CS, Borzutzky A, Vollmann EH, von Andrian UH, et al. Leucine-rich repeat containing 8A (LRRC8A) is essential for T lymphocyte development and function. *J Exp Med*. 2014; 211:929–42. [PubMed: 24752297]
4. Qiu Z, Dubin AE, Mathur J, Tu B, Reddy K, Miraglia LJ, et al. SWELL1, a plasma membrane protein, is an essential component of volume-regulated anion channel. *Cell*. 2014; 157:447–58. [PubMed: 24725410]
5. Voss FK, Ullrich F, Münch J, Lazarow K, Lutter D, Mah N, et al. Identification of LRRC8 heteromers as an essential component of the volume-regulated anion channel VRAC. *Science*. 2014; 344:634–8. [PubMed: 24790029]
6. Pedersen SF, Klausen TK, Nilius B. The identification of a volume-regulated anion channel: an amazing Odyssey. *Acta Physiol*. 2015; 213:868–81.
7. Cahalan MD, Lewis RS. Role of potassium and chloride channels in volume regulation by T lymphocytes. *Soc Gen Physiol Ser*. 1988; 43:281–301. [PubMed: 2479106]
8. Juntilla MM, Koretzky GA. Critical roles of the PI3K/Akt signaling pathway in T cell development. *Immunol Lett*. 2008; 116:104–10. [PubMed: 18243340]
9. Hoffmann EK, Lambert IH, Pedersen SF. Physiology of cell volume regulation in vertebrates. *Physiol Rev*. 2009; 89:193–277. [PubMed: 19126758]
10. Syeda R, Qiu Z, Dubin AE, Murthy SE, Florendo MN, Mason DE, et al. LRRC8 proteins form volume-regulated anion channels that sense ionic strength. *Cell*. 2016; 164:499–511. [PubMed: 26824658]
11. Lalouette A, Lablack A, Guenet JL, Montagutelli X, Segretain D. Male sterility caused by sperm cell-specific structural abnormalities in ebouriffe, a new mutation of the house mouse. *Biol Reprod*. 1996; 55:355–63. [PubMed: 8828840]
12. Bella J, Hindle KL, McEwan PA, Lovell SC. The leucine-rich repeat structure. *Cell Mol Life Sci*. 2008; 65:2307–33. [PubMed: 18408889]
13. von Heijne G. Membrane-protein topology. *Nat Rev Mol Cell Biol*. 2006; 7:909–18. [PubMed: 17139331]

Key messages

- LRRC8A is an essential component of the VRAC, which regulates cellular volume and is important for T-cell development and function.
- *ebo/ebo* mutant mice harbor a homozygous mutation that truncates the 15 terminal LRRs of LRRC8A and severely impairs VRAC activity but spares T-cell development and function.
- LRRC8A-dependent VRAC activity is dispensable for T-cell development and function.

**FIG 1.**

ebo mutation leads to truncation of the LRRC8A C-terminus while preserving protein expression. **A**, Sanger sequencing showing a 2-bp deletion (*delTG*) in exon 3 of *Lrrc8a* in *ebo/ebo* mice. **B**, Semiquantitative RT-PCR of *Lrrc8a* mRNA from splenocytes of WT and *ebo/ebo* mice. **C**, Immunoblot analysis of LRRC8A expression in splenocytes of WT and *ebo/ebo* mice using anti-LRRC8A₇₉₁₋₈₀₈ antibody. **D**, Comparison of amino acid sequence 87 to 104 in LRRC8A and the corresponding sequences in LRRC8 family member homologues. Amino acids shared between LRRC8 family members and LRRC8A are highlighted in yellow. **E**, Flow cytometric analysis of intracellular LRRC8A expression in CD3⁺ T cells of CD4 Cre *Lrrc8a*^{f/f} and C57BL/6 WT control mice (left panel) and *ebo/ebo* and FVB/N WT control mice (*right panel*) using anti-LRRC8A₈₇₋₁₀₄ antibody. Columns and bars represent means and SEMs. *ns*, Not significant. ****P* < .001, Student *t* test.

**FIG 2.**

Effect of the *ebo* mutation on mouse phenotype. **A**, Gross appearance at 8 weeks of age of *ebo/ebo*, *+ebo*, and WT littermate mice. **B**, Weight at 11 weeks of age of *ebo/ebo* ($n = 14$) and WT ($n = 15$) littermate mice. **C**, Kaplan-Meier analysis of survival of *ebo/ebo* and WT littermate mice ($n = 10$ from each group). **D**, Representative hematoxylin and eosin–stained tissue sections from salivary glands, livers, and kidneys of *ebo/ebo* mice and WT littermates ($n = 3$ per group, $\times 10$ magnification). Bars = 200 μm . Arrow shows tubular degeneration. Results in Fig 2C and D, are representative of 3 independent experiments, each with 1 mouse per strain. Columns and bars represent means and SEM. *ns*, Not significant. $*P < .05$, log-rank test.

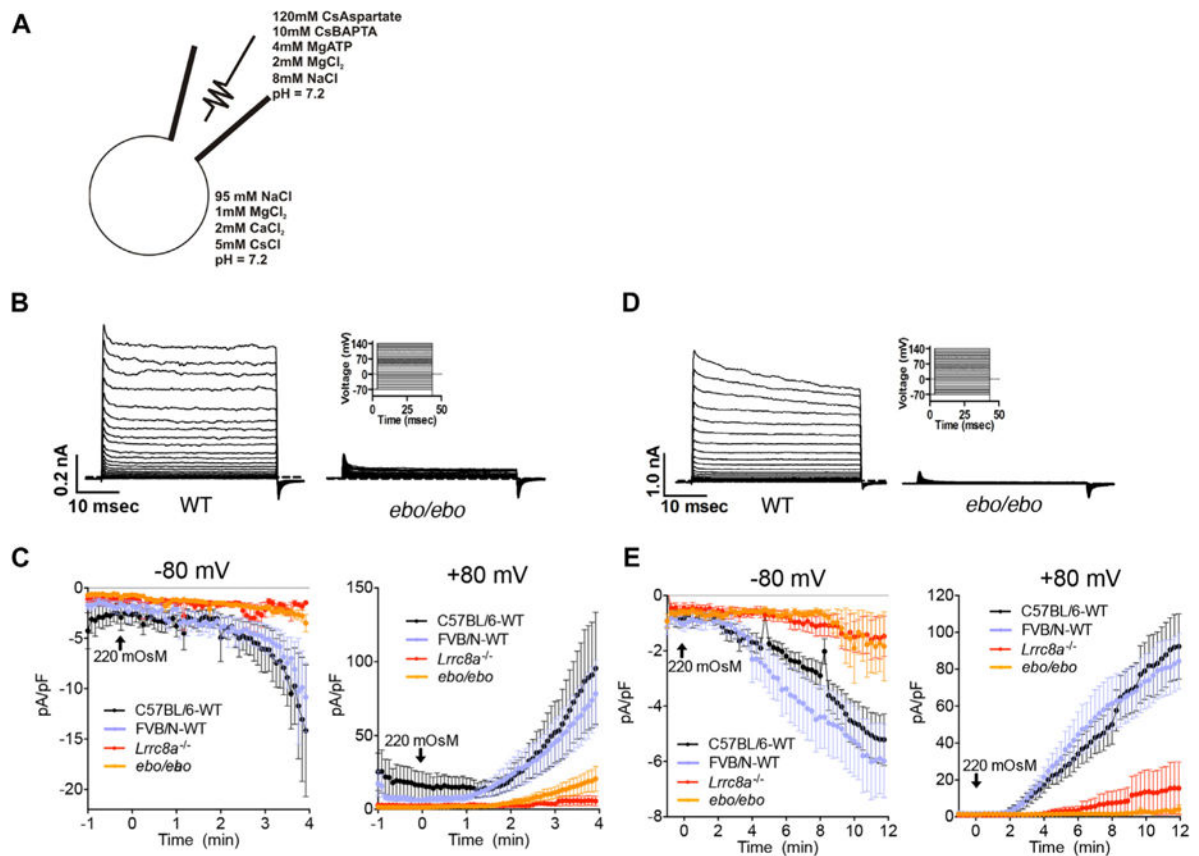
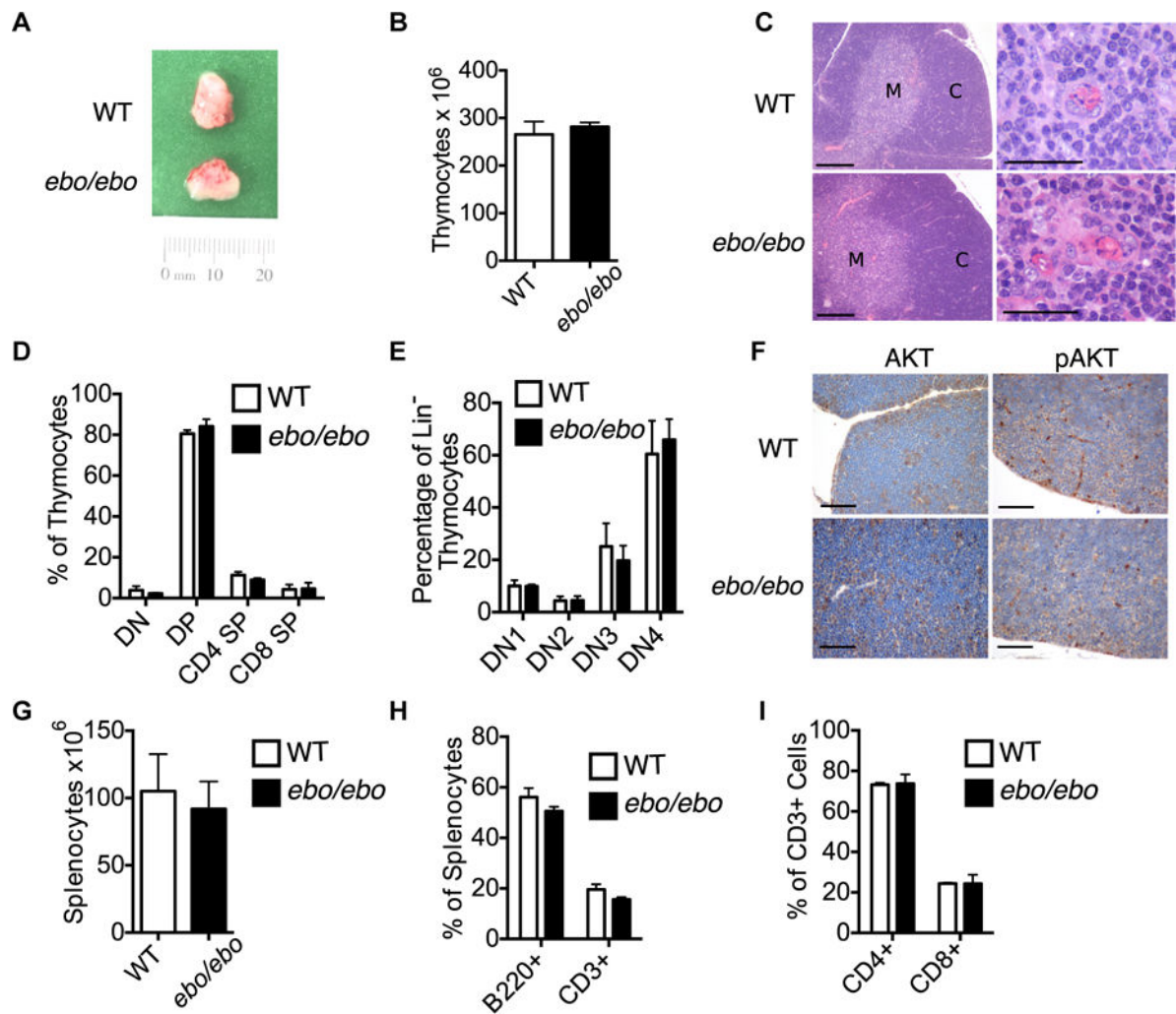


FIG 3. *ebo* dramatically reduces VRAC activity. **A**, Solution scheme used for patch-clamp analysis. **B** and **D**, Current traces induced in splenic T cells (Fig 3B) and peritoneal macrophages (Fig 3D) from WT (*left panels*) and *ebo/ebo* (*right lower panels*) mice by the indicated voltage step protocol shown in *right upper panels*. The dashed line indicates 0 current. **C** and **E**, Current densities induced in splenic T cells (Fig 3C) and peritoneal macrophages (Fig 3E) from *ebo/ebo*, *Lrrc8a*^{-/-}, and WT control mice by using a 220 mOsm hypotonic stimulus at -80 mV (*left panels*) or +80 mV (*right panels*). Results are representative of 8 to 12 cells pooled from 3 or more independent experiments by using 1 mouse per group in each experiment.

**FIG 4.**

Normal T-cell development and function in *ebo/ebo* mice. **A** and **B**, Gross appearance of the thymus (Fig 4A) and number of thymocytes (Fig 4B) in 3-week-old WT and *ebo/ebo* mice. **C**, Hematoxylin and eosin staining of thymi from WT and *ebo/ebo* mice (left panels: $\times 10$ magnification; bars, 200 μ m; right panels: medullary area $\times 60$ magnification; bars = 30 μ m). **C**, Cortex; **M**, medulla. **D**, Percentages of DN, double-positive, and single-positive thymocytes in 3-week-old WT and *ebo/ebo* mice. **E**, Percentages of DN1, DN2, DN3, and DN4 thymocytes in WT and *ebo/ebo* mice. **F**, AKT and phospho-AKT immunohistochemistry of thymi from WT and *ebo/ebo* mice ($\times 40$ magnification; bars = 50 μ m). **G-I**, Number of splenocytes (Fig 4G), percentages of CD3⁺ and B220⁺ cells (Fig 4H), and percentages of CD4⁺ and CD8⁺ cells (Fig 4I) in spleens from 11-week-old WT and *ebo/ebo* mice. Results in Fig 4, B, represent 4 mice per group pooled from 2 independent experiments. Results in Fig 4D and E, are of 1 representative experiment with 3 mice per group. Similar results were obtained in 2 additional experiments with 1 mouse per group. Results in Fig 4G, represent 9 mice per group pooled from 3 independent experiments. Columns and bars represent means and SEMs. Results in Fig 4H and I, represent 4 mice per group pooled from 2 independent experiments.

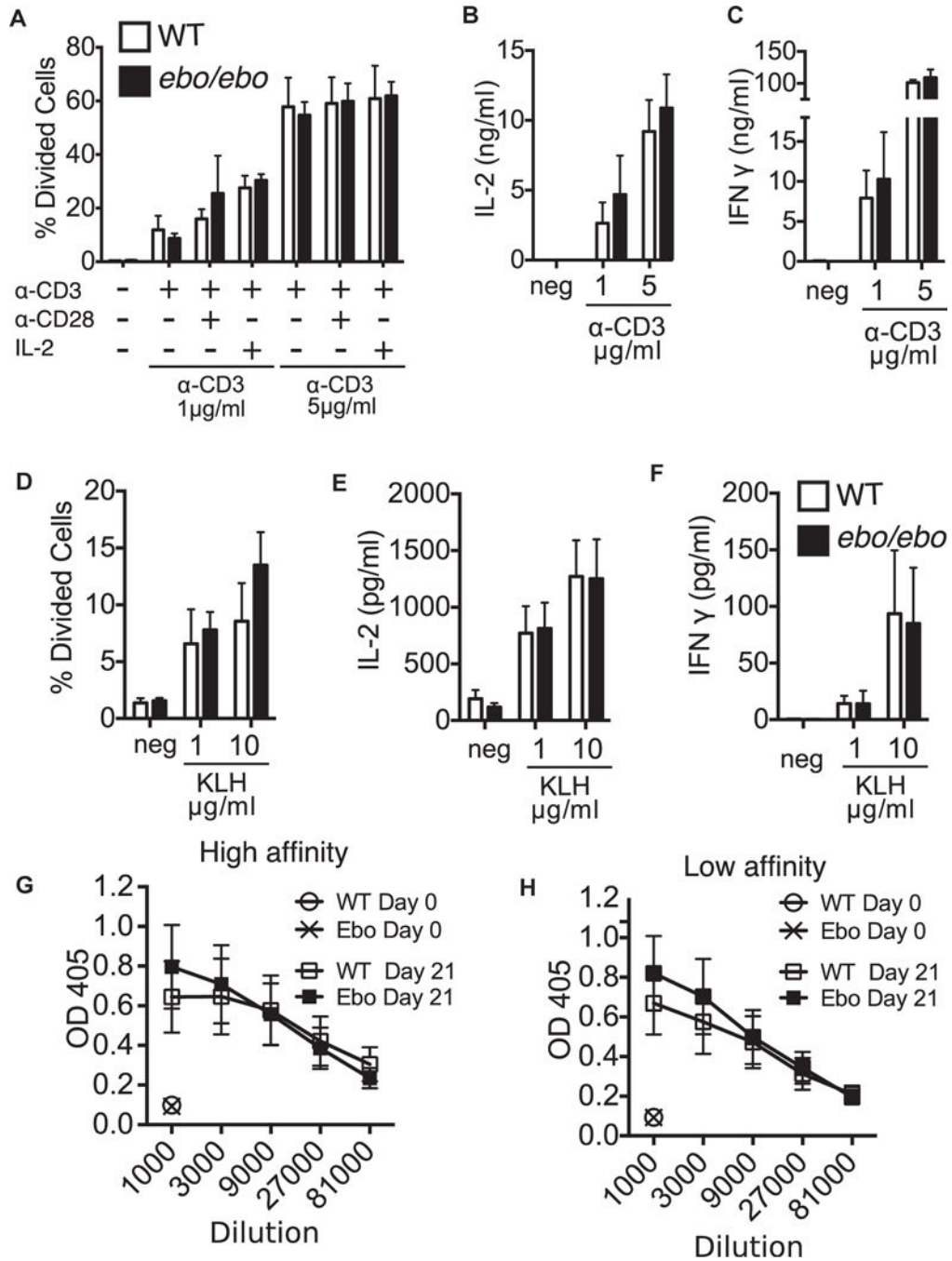


FIG 5. Normal T-cell function in *ebo/ebo* mice. **A–C**, Proliferation (Fig 5A) and secretion of IL-2 (Fig 5B) and IFN- γ (Fig 5C) by splenic T cells from WT and *ebo/ebo* mice in response to stimulation with immobilized anti-CD3 mAb, anti-CD3 plus anti-CD28 mAbs, or anti-CD3 mAb plus IL-2. **D–F**, Proliferation (Fig 5D) and secretion of IL-2 (Fig 5E) and IFN- γ (Fig 5F) by splenic T cells from WT and *ebo/ebo* mice in response to stimulation with KLH. High- and low-affinity TNP-specific serum antibody titers in KLH-TNP-immunized WT and *ebo/ebo* mice are shown. Results in Fig 5, **A–C**, are pooled from 1 experiment with 3

mice per group. Similar results were obtained in 3 other experiments with 1 mouse per group each. Results in Fig 5, *D–H*, are pooled from 3 experiments with 4 mice per group. *Columns/lines* and *bars* represent means and SEMs.

Author Manuscript

Author Manuscript

Author Manuscript

Author Manuscript

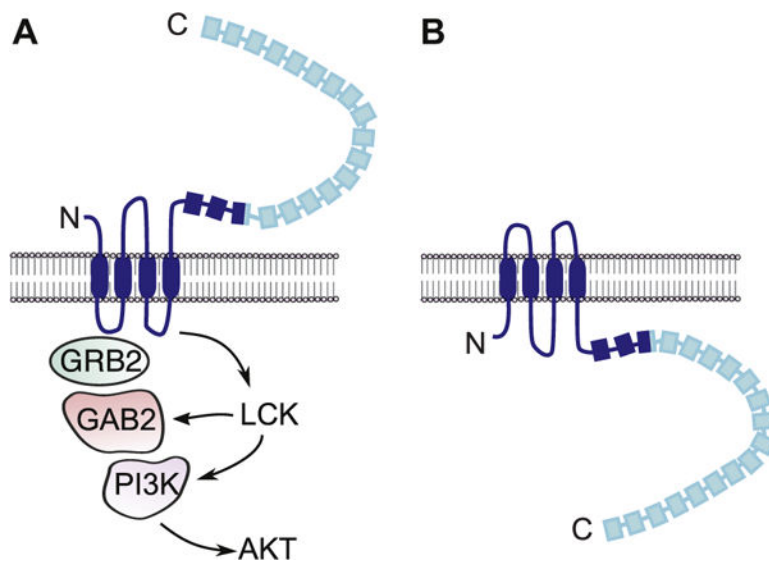


FIG 6. Schematic representation of the membrane topology of LRRC8A and interacting molecules. The 2 opposite orientations that LRRC8A potentially assumes (**A** and **B**) and their distinct roles in T-cell signaling (orientation **A**) and VRAC activity (orientation **B**) are shown. The LRRC8A region lacking in the *ebo* mutant is shown in light blue. *GAB2*, GRB2-associated-binding protein 2; *GRB2*, growth factor receptor-bound protein 2; *PI3K*, phosphoinositide 3-kinase.